объединенный
институт
ядерных
исследований
дубна

E2-94-337

S.V.Afanasiev, M.V.Altaisky, Yu.G.Zhestkov

ON APPLICATION OF WAVELET ANALYSIS TO SEPARATION OF SECONDARY PARTICLES FROM NUCLEUS-NUCLEUS INTERACTIONS

Submitted to «Il Nuovo Cimento»

1994

1 Introduction

The simplest way to tackle with almost any physical problem is to build a functional basis with the same symmetry as that of original problem or close to it. That's why the Bessel functions fit the problems with cylindrical symmetry, as well as spherical functions fit the SO_3 symmetrical ones. The application of this very idea to certain classes of stochastic processes found its implementation in wavelet analysis.

The Brownian motion

$$P(X(t) - X(t_0)) = \frac{1}{\sqrt{4\pi\mathcal{D}|t - t_0|}} \exp\left(-\frac{[X(t) - X(t_0)]^2}{4\mathcal{D}|t - t_0|}\right)$$

– one of the most common random processes – has long been known to be invariant under the scaling transformation (See e.g. [1] for details.)

$$P(b^{1/2}[X(bt) - X(bt_0)]) = b^{-\frac{1}{2}} P(X(t) - X(t_0)) \tag{1}$$

Therefore, it seems quite natural to use decomposition with respect to affine group

$$t' = \frac{t + b}{l}, \tag{2}$$

namely dilatations and translations, when studying Brownian motion, as well as other similar random processes.

Technically, decomposition is performed by convolution of function ψ with certain function $g(t)$, called wavelet, with the argument shifted to b and dilated by l. It is essential that function g has limit supporter. Therefore, unlike to the Fourier transform, which is inherently nonlocal, wavelet analysis or synthesis can be performed locally on a signal (field).

Based on the affine group representation, wavelet analysis and synthesis allow one to unfold a signal (a field), into space, time and direction. It works as a "microscope" discriminating different scales and a polarizer separating different angular contributions. Wavelet analysis has been applied to signal processing, image coding, turbulence data analysis and some other fields.

The numerous applications of wavelets to random data analysis (See e.g. [3] and references therein.) has proved it to be a powerful tool for studying fractal signals and data on cascading processes.

2 Definitions

As a decomposition based on an affine group

$$\vec{x} \to a\vec{x} + \vec{b},$$

wavelet transform (WT) of an arbitrary function $f(x)$ can be written as

$$|f\rangle = \int |a, b; g\rangle d\mu(a, b)\langle a, b; g|f\rangle \tag{3}$$

where

$$\begin{aligned} \langle a, b; g|f\rangle &\equiv T_g(l, b, \theta) = C_g^{-1} \int_{R^n} f(x) g^* \left[\Omega^{-1}(\theta)\frac{\vec{x} - \vec{b}}{l}\right] l^{-n} d^n x \\ C_g &= (2\pi)^n \int_{R^n} |\hat{g}(\vec{k})|^2 \frac{d^n k}{|k|^n} \end{aligned} \tag{4}$$

$$\hat{g}(\vec{k}) = (2\pi)^{-n} \int_{R^n} g(\vec{x}) e^{-\imath \vec{k}\vec{x}} d^n x \tag{5}$$

The rotation tensor Ω belongs to the group SO_n rotations in R^n and depends on the Euler angles θ. In terms of the Euler angles θ and scale (length) l the reconstruction formula (3) takes the form

$$f(x) = \int_0^\infty \frac{dl}{l^{n+1}} \int_{R^n} g\left\{\frac{x-b}{l}\right\} T_g[l,b,\theta] d^n b d\mu(\theta) \tag{6}$$

where

$$d\mu(\theta) = \prod_{s=1}^{n} \frac{\Gamma(\frac{s}{2})}{(2\pi)^{(s/2)}} \prod_{k=1}^{n-1} \prod_{j=1}^{k} \sin^{j-1}\theta_j^k d\theta_j^k$$

is the SO_n invariant measure.

It should be noted that an arbitrary fun^ction $g(x)$ cannot be used as a wavelet in general: the admissibility condition (4), which guarantees the existence of inverse transformation (3), is required.

Historically, the wavelet transform originated from Morlet's work [4] on seismic data analysis and Zimin's [5] hierarchical basis for turbulence. Since these first works a lot of studies has been done with different wavelet functions $g(x)$, because the admissibility condition allows a wide variety of functions: condition (4) practically means $\hat{g}(\vec{k}=0)=0$. The most common chois of real wavelets, however, is restricted to the derivatives of Gauss

$$g_m(x) = (-1)^m \frac{d^m}{dx^m} e^{-\frac{x^2}{2}}, \qquad \hat{g}^m(k) = (\imath k)^m e^{-\frac{k^2}{2}} \tag{7}$$

Besides, one can also use complex-valued functions as wavelets [6, 8].

3 Detection of random signal singularities with wavelets

Wavelets has long been known as an attractive tool for analyzing function regularity [7, 8] as well as for searching singularities of random signals [9]. The latter application is significant for all kinds of spectrum recognition. A very instructive example of wavelet application to singular measures is the reconstruction of singularity spectrum from so-called "devil staircase" measure (See e.g. [3] and references therein.).

The basic idea of the method is the following. Let us consider a measure $\mu(x)$ (with $x \in R^1$ for simplicity). Then, considering the integral measure

$$s(x) = \int_0^x d\mu(x), \tag{8}$$

one can use the following theorem [10]:

Theorem 1 *If $s(x)$ is a bounded locally integrable function that satisfies*

$$s(x) - s(x_0) = O(|x - x_0|^h), \qquad h \in [0, 1]$$

at some point $x_0 \in \mathrm{R}$, then, provided the analyzing wavelet satisfy $g \in \mathrm{L}^1$, $\quad x^h g \in \mathrm{L}^1$ and the zero-mean condition

$$\int g(x)dx = 0,$$

its wavelet transform behaves as

$$T_g(a, x) = O(a^h + |x - x_0|^h)$$

Thus, a way to detect a singularity is to investigate the decay rate of the amplitude of wavelet transform

$$T_g(a, x) = O(a^h) \tag{9}$$

in the influence cone of singularity

$$|x - x_0| \leq const \cdot a.$$

which can be naturally done by log – log plotting of $T_g(a, x)$.

4 On possible applications of wavelets in nuclear physics

Up to now the most common applications of WT belonged to either turbulence data analysis, where scaling is an inherent feature of fluid physics, or to image processing, where the singularity detection and local reconstruction are significant. The only known applications of WT to physics beyond turbulence, at least to the authors' knowledge, are related to spectra analysis. Such a situation seems to be rather strange for a number of reasons.

- Firstly, since the works of Zimin, WT proved to work efficiently in situations where cascade processes play significant role. Therefore, if the measure $\mu(x)$ describes an event number at certain point x, ($x \in R^3$ in general), then the search for *jet* events can be performed with the aid of WT, in a way similar to "devil staircase" singularity reconstruction (See e.g. [3, 9] for details.)

- Secondly, if x is regarded as time (or energy), WT works as a tool for studying time (or energy) scaling of the process described by time (or energy) event density $\mu(x)$.

- Thirdly, being local in both x and Fourier space, WT can provide more information in spectral problems, where Fourier methods fail or work insufficiently.

- The contributions of different frequency bands to WT are kept reasonably separated. This separation is achieved with quite insignificant loss of resolution in time variable (if a signal is considered). That's why the reconstruction is "robust" in the sense of being stable under small perturbations, which enables one to distinguish between "usefull" low bands (in Fourier space) and contributions of close high frequencies $\omega_1 - \omega_2 \approx 0$ usually generated by the noise.

The situation turns to be even more strange if we take into account the well-known facts related to *Local Parton Hadron Duality* [11], i.e. the similarity between momentum spectra of hadrons and those of partons. This similarity, which is closely related to n-parton correlations and multiplicity moments behavior in phase space, has been studied in [12]. The fractal behavior of final multiparton states [14] was studied by several authors. They calculated the fractal dimension directly from multiplicity distribution moments and study the entropy of secondary particles

$$S = -\sum_n P_n \ln P_n.$$

where P_n is the probability of having "n" produced particles in the final state [15]. They found the scaling behavior, but, as the method was rather rude (see [3] for the shortcomings of the fractal dimension calculations without wavelets), the rare but interesting events can be lost. Besides, the fractal analysis of multiparticle production in hadron-hadron collisions has been recently done by other authors [13].

That's why we are going to apply wavelet methods for separation of secondary particles (K mesons, in particular) in $d+Au$ interactions.

5 Secondary particle separation as an image recognition problem

The aim of the present paper is not to cover all the problems mentioned above with the aid of wavelet analysis. In this preliminary study we just show its facilities for energy versus time of flight data (Fig.1) obtained from $d + Au \to \ldots$ reactions in experiments carried out at the Nuclotron using the internal target at deuteron momentum of $3.8 GeV/c$ in March 1994.

The following detectors operated at present run:
Two identical telescopes containing four scintillation counters each with $2 \times 2 \times 0.5\ cm^3$, $3 \times 3 \times 0.5\ cm^3$, $4 \times 4 \times 0.5\ cm^3$ and $7.5 \times 7.5 \times 65\ cm^3$, respectively. The first three counters aimed for ΔE and TOF measuremets, and the last one for the measurement of charge particle energy E. The on-line scatter plot of TOF vs Energy loss in Fig.1 qualitatively demonstrates the π, p, d, t and He separation capability.

In Fig.2 we present the mass spectrum obtained from the primary data by the standard method of comparing the time of flight and the energy

$$\beta = \frac{v}{c} = \frac{l}{tc} = \sqrt{\frac{E^2 - m^2}{E^2}} \qquad (10)$$

Due to the presence of both $\pi-$mesons and protons, which dominate, in the central (dark, see Figs.1,3) region of the plot ($E \sim 250$ MeV), which contains the largest part of the registered particles, it is difficult to distinguish other events in this region. Besides, high energy protons ($E > 400$ MeV) due to decreasing energy loss give contribution mainly to the low energy region about 200 MeV.

6 Algorithm

The main idea of implying a wavelet analysis to investigation of events in nuclear and high energy physics is to use its good properties in separating events from noise. Using wavelet one can look at experimental data with various resolution. This can be used to searching for tracks of particles and different kind of events, e.t.c.

To use a multiresolution analysis [16] one should choose a family of closed subspaces $V_m \subset L^2(R), m \in Z$, such that

1. $f(x) \in V_m \Leftrightarrow f(2*x) \in V_{m-1}$
2. $\ldots \subset V_2 \subset V_1 \subset V_0 \subset V_{-1} \subset V_{-2} \subset \ldots$
   $\cap V_m = 0, \cup V_m = L^2(R)$
3. there is a $\phi \in V_0$ such that its linear integer translations $\phi_{0n}(x) = \phi(x+n)$ constitute a basis in V_0 (consequently, functions ϕ_{mn} constitute a basis in V_m).
4. there exist $0 < A \leq B < \infty$, such that for all $(c_n)_{n \in Z} \in l^2(Z)$, $A\sum_n |c_n|^2 \leq ||\sum_n c_n \phi_n^m||^2 \leq B\sum_n |c_n|^2$.

The orthogonal projections of a function which we analyse on a chain of subspaces V_m represent snapshots of this function with different resolution. Choosing an appropriate basic function ϕ, one could select different kinds of snapshots.

To make the decomposition close, one should also define a chain of subspaces W_m ortogonal to V_m, such that

$$V_{m-1} = V_m \oplus W_m. \tag{11}$$

The coefficients of a projection on V_m and W_m are

$$\begin{aligned} s_n^m &= \int f(x)\phi_n^m(x)dx, \\ d_n^m &= \int f(x)\psi_n^m(x)dx. \end{aligned} \tag{12}$$

where in a discrete case a sum is implied. For the simplest case of Haar wavelet (See e.g. [16]) the basic functions are:

$$\phi_k^j(x) = \begin{cases} |I_k^j|^{-1/2} & \text{for } x \in I_{j,k} \\ 0 & \text{elsewhere} \end{cases} \tag{13}$$

$$\psi_k^j(x) = \begin{cases} 2^{-j/2} & \text{for } 2^j(k-1) < x < 2^j(k-1/2), \\ -2^{-j/2} & \text{for } 2^j(k-1/2) \le x < 2^j k, \\ 0 & \text{elsewhere} \end{cases} \tag{14}$$

The I_k^j denotes the supporter of j-th level basic functions

$$I_j \equiv I_k^j = [2^j(k-1), 2^j k].$$

The approximate reconstruction formula has the form

$$P_m f = \sum_n s_n^m \phi_n^m + \sum_n d_n^m \psi_n^m \tag{15}$$

In our two-dimensional problem we used a pyramidal scheme with a basis taken in the form of a tensor product

$$h_{I \times J} = (\psi_I \oplus \phi_{I'}) \otimes (\psi_J \oplus \phi_{J'}),$$

or explicitly,

$$\{h_1, h_2, h_3\} = \{\psi_I(x)\psi_{I'}(y), \psi_I(x)\phi_{I'}(y), \phi_I(x)\psi_{I'}(y)\}. \tag{16}$$

The corresponding coefficients can be easily derived from the formulae (12):

$$\begin{aligned}
s^{j+1}_{k_x,k_y} &\sim s^j_{2k_x-1,2k_y-1} + s^j_{2k_x-1,2k_y} + s^j_{2k_x,2k_y-1} + s^j_{2k_x,2k_y} \\
d^{j+1}_{(1);k_x,k_y} &\sim s^j_{2k_x-1,2k_y-1} - s^j_{2k_x-1,2k_y} - s^j_{2k_x,2k_y-1} + s^j_{2k_x,2k_y} \\
d^{j+1}_{(2);k_x,k_y} &\sim s^j_{2k_x-1,2k_y-1} - s^j_{2k_x,2k_y-1} + s^j_{2k_x-1,2k_y} - s^j_{2k_x,2k_y} \\
d^{j+1}_{(3);k_x,k_y} &\sim s^j_{2k_x-1,2k_y-1} + s^j_{2k_x,2k_y-1} - s^j_{2k_x-1,2k_y} - s^j_{2k_x,2k_y},
\end{aligned}$$

where s^0 stand for the primary data.

7 Results

The primary data $E - dt$ plot for the above mentioned run is shown in Fig.1. The X-axis corresponds to ADC channel numbers, Y-axis to TDC ones. (Both axes are scaled by factor 1). In this plot, over a noisy background we can distinguish two contrast regions: the upper, which corresponds to secondary protons, and the lower, which corresponds to π-mesons.

To clear out the contribution of dominating processes we performed the wavelet analysis. Having calculated the wavelet image (the Haar wavelet was used) of the initial data plot we substracted the central domain, in which $d^{(2)}$ coefficients (See Fig.4) practically wanish.

The resulting mass spectrum is presented in fig.5. We identify the central peak near 500 MeV, clearly distinguished on mass histogramm with the K-mesons contribution.

Besides, sequentially scaling the picture, we can clearly distinguish 4 regions:

- upper right region: secondary deuterons
- two above-mentioned regions
- a K-meson branch.

***

The authors are grateful to Dr. V.Kolesnikov for invaluable technical aid in data acquisition. We are also grateful to prof. S.Ratti for stimulating discussions. One of the authors (S.A.) is grateful to Russian Fund for Fundamental Research, grant 93-02-3773, for financial support.

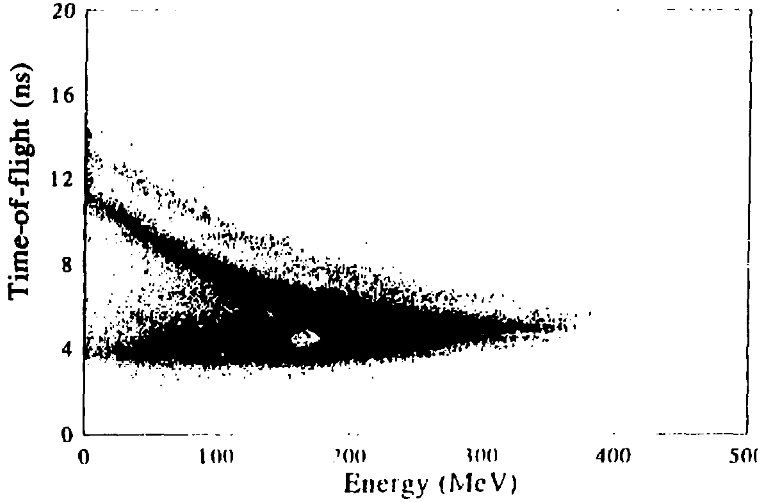

Fig. 1 TOF vs E plot of primary experimental data.

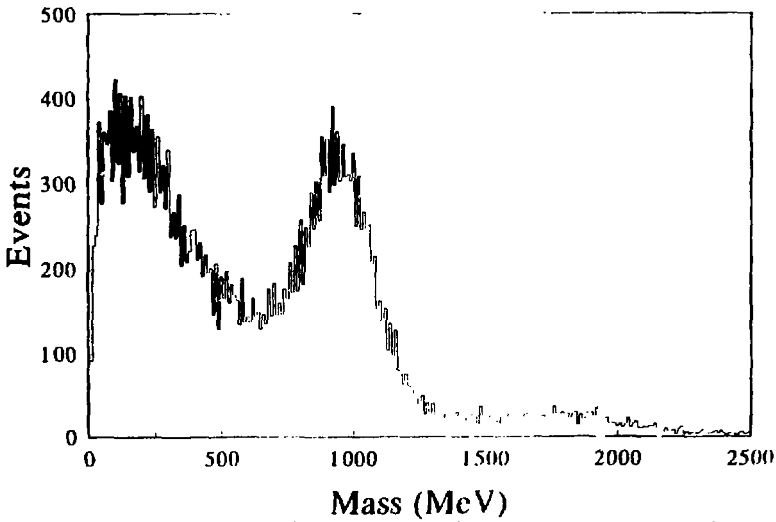

Fig. 2 Spectrum of reconstructed mass from primary data.

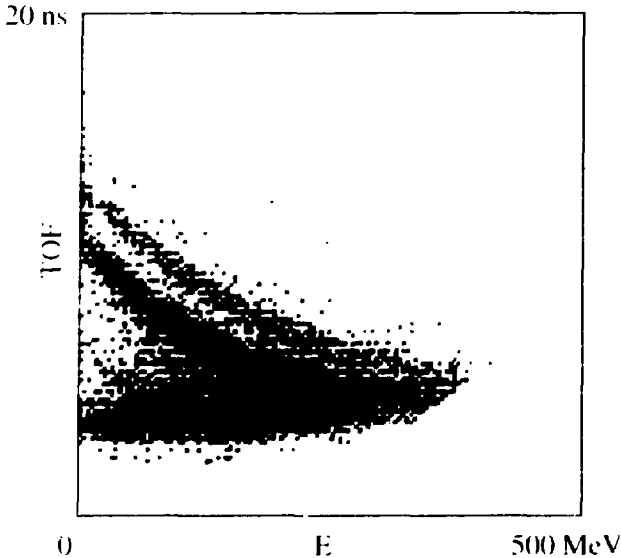

Fig. 3 $s^{(1)}$ coefficients plot for the data set of Fig. 1.

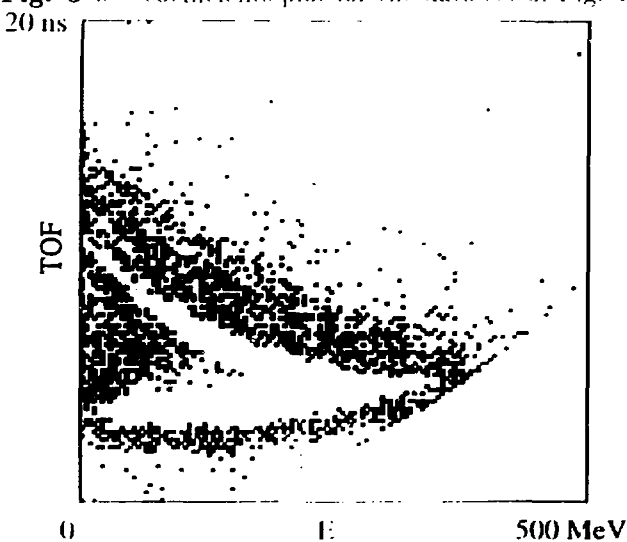

Fig. 4 $|d^{(1)}|$ coefficients plot for the data set of Fig. 1.

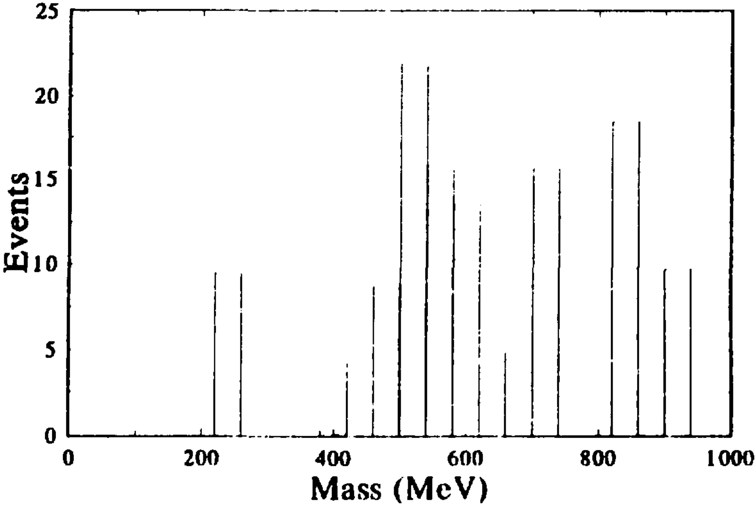

Fig. 5 Mass spectrum obtained after filtering.

References

[1] Feder, J., Fractals, Plenum Press, New York, 1988.

[2] Daubechies, I., Grossmann, A., Meyer, Y., J. Math. Phys. 27(1986)1271

[3] Muzy J.F., Bacry, E., Arneodo. A., Phys. Rev. Lett 67(1991)3515
Muzy J.F., a.o. Phys. Rev. E47(1993)875

[4] Morlet, J. 1981. Sampling theory and wave propagation. Proc. 51st Annu. Meet. Soc. Explor. Geophys., Los-Angeles.

[5] Zimin V.D., Izv. Atmos. Ocean. Phys. 17(1981)941 (in Russian)

[6] Paul T., J. Math. Phys. 25(1984)3522

[7] Holshneider, M., J. Stat. Phys. 50(1988)963

[8] Grossmann, A., Holshneider, M., Konland-Martinet, R. and Morlet, J., in *Inverse Problem*, ed. by P. C. Sabatier, Advances in Electronics and Electron Physics, Supplement 19, Acad. Press, Orlando, 1987.

[9] Combes J.M., Grossmann, A. and Tchamitchan, P., eds., Wavelets, Springer, Berlin, 1988.

[10] Holshneider, M. and Tchamitchan, P., in *Les Ondelcts*, ed by Lemarie, P.G., Springer, Berlin, 1990.

[11] Ya.I. Azimov, Yu.L. Dokshitzer, V.A. Khoze, S.I. Troyan, Z. Phys. C27(1985)65, *ibid.* C31(1986)231

[12] Ochs W., Wosiek J., Phys. Lett. B305(1993)144

[13] Boca G., a.o. Nuovo Cim. A105(1992)865

[14] G.Gustafson and A.Nilson Z. Phys. C52(1991)533

[15] A.Mikhopadhyay, P.L. Jain, and G.Singh, Phys. Rev. C47(1993)410

[16] Daubechies I., Comm. Pure. Apl. Math. 16(1988)909

[17] Beylkin G., Coifman R. and Rokhlin V., Comm. Pure. Apl. Math. 44(1991)141

Received by Publishing Department
on August 18, 1994.